TRANSACTION ON CONTROL AND MECHANICAL SYSTEMS, VOL.1, NO.1, PP. 43-48, MAY, 2012.
TSEST Transaction Series on Engineering Sciences and Technologies

Unsteady Flow past a Flapping Aerofoil

K. Siva Kumar[1,✉] and Sharanappa V. Sajjan[2]

***Abstract*: Unsteady flow computations are presented for low speed Mach number flow past a combined pitching and plunging aerofoil. The Implicit Reynolds-averaged Navier-Stokes solver used for obtaining time-accurate solutions is based on finite volume nodal point spatial discretization scheme with dual time stepping. Results are obtained in the form of aerodynamic coefficients, time – averaged thrust coefficient and propulsion efficiency which agree well with the available results.**

Keywords: unsteady flow, RANS solver, implicit method, dual time stepping, pitching and plunging aerofoil.

1. INTRODUCTION

Unsteady flows are encountered in many aerospace applications and prediction of unsteady air loads plays a vital role in aircraft and helicopter design [1-3]. Since wind tunnel testing of unsteady flow situations is difficult and expensive, computational studies of wing stall, dynamic stall, blade-vortex interaction of helicopter rotors and aeroelastic problems like flutter, buffeting and gust-response etc., can provide important design data.

Flying birds usually flap their wings to generate both lift and thrust. Flapping motion of birds has a coupled pitching and plunging oscillation with some phase difference between them. Recent experimental and computational studies investigated the kinematics, dynamics, flow characteristics of flapping wings and shed some light on the lift, drag, and propulsive power considerations [4-5]. Yang et al. [6] have computed a sinusoidal pitching and plunging NACA 0012 aerofoil in a uniform stream of low speeds for different motion parameters by using inviscid version of a three-dimensional unsteady compressible Euler/Navier-Stokes flow solver and optimized for high propulsive efficiency and for high time-averaged thrust coefficient. Theodorsen [7] has developed compact expressions for forces and moments of a flapping flat plate aerofoil for small perturbed inviscid and incompressible flow. In the prediction of unsteady pressure distributions over aerofoils, the steady-state Kutta-Joukowsky condition is assumed. The flow is treated in two classes: the non circulating flow due to the aerofoil vertical acceleration and the circulatory flow due to the wake vortices. Many important features of flapping aerofoil behavior are depicted by the classical linear theory. The thrust force experienced by the flapping aerofoil was given by Garrick [8]. Tuncer and Platzer [9] used a compressible Navier-Stokes solver to compute the unsteady turbulent flow fields and obtained high propulsive efficiency when the flow remains mostly attached over the aerofoil oscillated in plunge and pitch. Isogai et al. [10] performed Navier-Stokes simulations of flow over a NACA 0012 aerofoil undergoing combined pitching and plunging motion at Re = 10^5. Ramamurti and Sandberg [11] performed numerical simulation of the flow over a flapping NACA 0012 aerofoil using a finite element incompressible Navier-Stokes solver at a Reynolds number of 1100. They found that the critical parameter which affects the thrust generation is kh rather than k. They also found that maximum thrust is obtained when the pitching motion leads the plunging motion by 120^o and the maximum propulsive efficiency occurs at Ø = 90^o. Anderson et al. [12] measured the time-averaged thrust coefficient, input power coefficient, and propulsion efficiency of a NACA 0012 aerofoil undergoing combined sinusoidal plunging and pitching motion in the testing tank facility at MIT.

This work was supported by the Council of Scientific and Industrial Research - National Aerospace Laboratories, *Bangalore, Karnataka, India.*

[1,2]*Computational and Theoretical Fluid Dynamics division, Council of Scientific and Industrial Research - National Aerospace Laboratories, Bangalore, Karnataka - 560017, India* ([1]shivak@ctfd.cmmacs.ernet.in) ✉, ([2]svsajjan@ctfd.cmmacs.ernet.in).

2. IMPRANS SOLVER

The solver is based on an implicit finite volume nodal point spatial discretization scheme with dual time stepping. Inviscid flux vectors are calculated by using the flow variables at the six neighboring points of hexahedral volume. Turbulence closure is achieved through the algebraic eddy viscosity model of Baldwin and Lomax.

The Reynolds-averaged Navier-Stokes equations for two-dimensional unsteady compressible flow in a moving domain in non-dimensional conservative form are given by

$$\frac{\partial U}{\partial t}+\frac{\partial F}{\partial x}+\frac{\partial G}{\partial y}=\frac{\partial V}{\partial x}+\frac{\partial W}{\partial y} \tag{1}$$

Where

$$U=\begin{bmatrix}\rho\\ \rho u\\ \rho v\\ e\end{bmatrix},\quad F=\begin{bmatrix}\rho(u-x_t)\\ \rho u(u-x_t)+p\\ \rho v(u-x_t)\\ e(u-x_t)+pu\end{bmatrix},\quad G=\begin{bmatrix}\rho(v-y_t)\\ \rho u(v-y_t)\\ \rho v(v-y_t)+p\\ e(v-y_t)+pv\end{bmatrix} \tag{2}$$

RECEIVED: 4, APR., 2012; **REVISED:** 18, MAY, 2012; **ACCEPTED:** 30, MAY, 2012; **PUBLISHED:** 30, JUN., 2012.

0101010043004820120000029

$$V = V_1(U, U_x) + V_2(U, U_y) = \frac{1}{Re_\infty}\begin{bmatrix} 0 \\ \lambda(u_x + v_y) + 2\mu u_x \\ \mu(v_x + u_y) \\ \mu v(u_y + v_x) + \lambda u(u_x + v_y) + 2\mu u u_x + \dfrac{\mu T_x}{(\gamma-1)M^2_\infty Pr} \end{bmatrix} \quad (3)$$

$$W = W_1(U, U_x) + W_2(U, U_y) = \frac{1}{Re_\infty}\begin{bmatrix} 0 \\ \mu(u_y + v_x) \\ \lambda(u_x + v_y) + 2\mu v_y \\ \mu u(u_y + v_x) + \lambda v(u_x + v_y) + 2\mu v v_y + \dfrac{\mu T_y}{(\gamma-1)M^2_\infty Pr} \end{bmatrix} \quad (4)$$

Here x and y are the Cartesian coordinates and t is the time variable; x_t and y_t are the Cartesian velocity components of the moving domain. For a fixed domain, the grid speeds x_t and y_t are zero. U is the vector of conserved variables; F, G are inviscid flux vectors and V, W are viscous flux vectors.

The primitive variables are density ρ, velocity components u, v in the x and y directions, pressure p, temperature T and total energy e per unit volume. The non-dimensional variables used in the above equations have been obtained by using the following free stream values as reference quantities: ρ_∞(density),U_∞(velocity), μ_∞ (viscosity), $\rho_\infty U^2_\infty$(pressure), T_∞(temperature), and so on. Some characteristic length such as chord c of an aerofoil is chosen as the length scale.

M_∞ and Re_∞ are the free stream Mach number and Reynolds number respectively; γ is the ratio of specific heats and Pr is the Prandtl number. In addition, the viscosity coefficients λ and μ given by the Stokes relation

$$3\lambda + 2\mu = 0 \quad (5)$$

and the Sutherland's law of viscosity

$$\mu = C_1\left[\frac{T^{3/2}}{T + C_2}\right] \quad (6)$$

For turbulent flows, the laminar viscosity coefficient μ is replaced by $\mu + \mu_t$, and μ/Pr is replaced by $\mu/Pr + \mu_t/Pr_t$; the turbulent viscosity coefficient μ_t and the turbulent Prandtl number Pr_t are provided by a turbulence model. Finally the system is closed using the perfect gas equation of state in non-dimensional form as

$$P = \frac{\rho T}{\gamma M^2_\infty} \quad (7)$$

The Euler equations for inviscid flow are obtained from the Navier-Stokes equations by setting

$$\frac{1}{Re_\infty} = 0$$

A. Computational method

Applying Euler's implicit time differencing formula [13]

$$U^n = U^{n+1} - \left(\frac{\partial U}{\partial t}\right)^{n+1}\Delta t + O\left(\Delta t^2\right) \quad (8)$$

to the governing (1), we obtain

$$\Delta U^n + \Delta t\left[\frac{\partial}{\partial x}(F - V) + \frac{\partial}{\partial y}(G - W)\right]^{n+1} = 0 \quad (9)$$

Here U^n = U (t) = U (n Δt) is the solution vector at time level n and $\Delta U^n = (U^{n+1} - U^n)$ is the change in U^n over time step Δt. In order to facilitate the finite volume formulation, the above equations are written in the integral form as

$$\iint_\Omega \Delta U^n dxdy + \Delta t\int_\Gamma\left[(F - V)^{n+1}dy - (G - W)^{n+1}dx\right] = 0 \quad (10)$$

where Ω is any two-dimensional flow domain and Γ is the boundary curve.

In the nodal point finite volume approach [14-15], the flow variables are associated with each mesh point of the grid and the integral conservative equations are applied to each control volume obtained by joining the centroids of the four neighbouring cells of a nodal point. Application of nodal point spatial discretization to (10). leads to the following equations for the computational cell Ω_{ij}

$$\Delta U^n_{ij} h_{ij} + \Delta t\int_{\Gamma_{ij}}\left[(F - V)^{n+1}dy - (G - W)^{n+1}dx\right] = 0 \quad (11)$$

Linearzing the changes in flux vectors using Taylor's series expansions in time and assuming locally constant transport properties, (11). can be simplified to

$$\Delta U^n_{ij} + \frac{\Delta t}{h_{ij}}\left[\int_{\Gamma_{ij}}\left\{A^n - \frac{\partial}{\partial x}R^n\right\}\Delta U^n dy - \int_{\Gamma_{ij}}\left\{B^n - \frac{\partial}{\partial y}S^n\right\}\Delta U^n dx\right] = -\frac{\Delta t}{h_{ij}}\left[\int_{\Gamma_{ij}}(F - V)^n dy + \int_{\Gamma_{ij}}(G - W)^n dx\right] \quad (12)$$

Here A, B, R and S are the Jacobian matrices which are given by

$$A = \frac{\partial F}{\partial U}, B = \frac{\partial G}{\partial U}, R = \frac{\partial V_1}{\partial U_x} \text{ and } S = \frac{\partial W_2}{\partial U_y} \quad (13)$$

This RANS solver has been extensively validated for computing unsteady flow past pitching aerofoils and wings [16], helicopter rotor blades [17-18], wind turbines [19] etc. Here, the solver has been applied for computing two-dimensional unsteady compressible viscous flow over combined pitching and plunging NACA 0012 aerofoil.

3. GRID GENERATION

For all present computations, the structured C-type grid, of size 247×65 (stream-wise × normal) moving with combined pitching and plunging NACA 0012 aerofoil is used which is shown in Fig. 1. The grid points are properly clustered near the leading, trailing edges and wall normal direction. The close-up view of the grid is shown in Fig. 2.

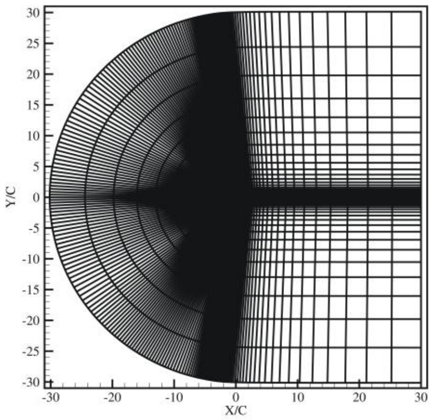

Fig.1. C- Grid around the NACA 0012.

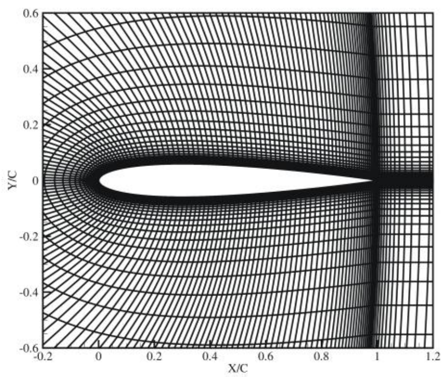

Fig.2. Close-up view of the aerofoil grid.

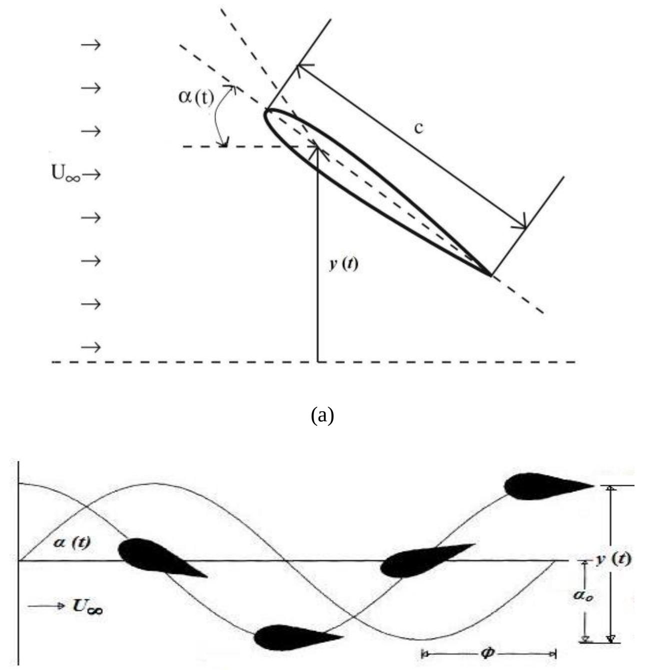

Fig.3. (a) Aerofoil in combined pitching and plunging motion (b) Aerofoil in combined pitching and plunging motion for a phase angle Ø = 90°.

4. FLAPPING MOTION OF THE AEROFOIL

The sinusoidal motion of combined pitching and plunging aerofoil is defined by the following expressions. The plunging motion of the aerofoil is

$$y(t) = y \sin(\omega t) \quad (14)$$

where t is physical time, ω and y are the angular frequency and the amplitude of the plunging oscillation respectively, y is positive in the upward direction. The non-dimensional time, $\tau = U_\infty t / c$, amplitude in plunge, $h_a = y / c$, and the reduced frequency, $k = \omega c / 2U_\infty$. Then the instantaneous non-dimensional plunging velocity of the aerofoil is given by

$$\dot{y} / U_\infty = 2kh_a \cos(2k\tau) \quad (15)$$

The coupled pitching oscillation is defined as rotating about a pivot point on the aerofoil chord which is shown in Fig. 3 (a). The instantaneous angle measured clockwise from the mean chord is $\alpha(t)$ which is given by

$$\alpha(t) = \alpha_m + \alpha_o \sin(\omega t + Ø) \quad (16)$$

The instantaneous non-dimensional pitching velocity of the aerofoil is given by

$$\dot{\alpha} / U_\infty = 2k\alpha_o \cos(2k\tau + Ø) \quad (17)$$

where α_o is the amplitude of pitching oscillation, α_m is the mean angle of attack and $Ø$ is the phase angle ahead of the plunging motion which is shown in Fig. 3 (b).

The mean thrust coefficient and propulsion efficiency are computed using the following expressions

The mean thrust coefficient is defined as

$$(\bar{C}_t) = -\bar{C}_d + (C_d)_{stat} \quad (18)$$

where $\bar{C}_d$ is the mean drag coefficient, averaged for one flapping period. $(C_d)_{stat}$ is the steady drag of the non-moving wing at its present mean angle of attack.

The propulsion efficiency can be calculated from the ratio between power output and power input, in this case which is given by

$$(\eta_{prop}) = (\bar{C}_t) / (\bar{C}_p) \quad (19)$$

where C_p instantaneous power input coefficient is given by

$$C_p = -(C_l \cdot \dot{y} / U_\infty + C_m \cdot c\, \dot{\alpha} / U_\infty) / U_\infty \quad (20)$$

5. RESULTS AND DISCUSSION

The computations have been carried out for two-dimensional unsteady viscous flow over a combined pitching and plunging aerofoil at low Mach number. For all simulations, steady state solutions are first obtained. After steady state convergence is reached, the aerofoil is then undergoes a prescribed sinusoidal motion, both pitching about half chord and plunging motion. Five consecutive cycles were computed to obtain periodic solutions.

Computation is carried out for 0^o mean angle of attack with $M_\infty = 0.1$, $Re_\infty = 2.41 \times 10^6$, $k = 0.27$, $\alpha_0 = 30^o$, non-dimensional plunge amplitude of 1.25 and with a leading phase angle of 90^o between pitching and plunging motion. The time step $\Delta t = 0.005$ was used for all computations. Fig. 4 and Fig. 5 represent the instantaneous lift, pitching moment and thrust coefficient versus y/c for a pitching-plunging NACA 0012 aerofoil. The computed loops of the aerodynamic coefficients clearly demonstrate the hysteretic property existing between the up-stroke and down-stroke. The lift and the pitching moment values are higher during down stroke than during up stroke. The thrust coefficient values are smaller during the first half of up stroke compared to the second half of down stroke and become higher during the second half of up stroke than during the first half of down stroke. The difference in predicted values and the values of Euler solutions of Yang et al. [6] is probably due to the presence of viscous effect in the present simulations. For further validation we have computed two cases as Case 1 and Case 2. The time-averaged thrust coefficient and propulsion efficiency values for both the cases are compared with the available results, which are discussed in the following sections.

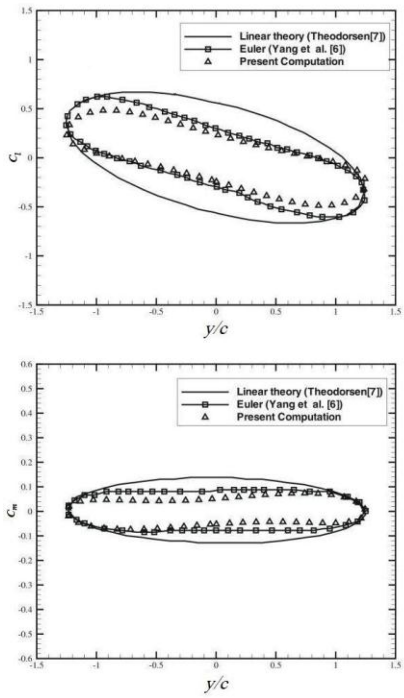

Fig.4. The variation of lift and moment coefficients with heave distance for NACA 0012 aerofoil at 0o mean angle of attack.

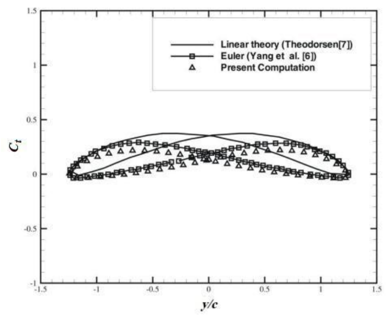

Fig.5. The variation of thrust coefficient with heave distance for NACA 0012 aerofoil at 0o mean angle of attack.

Case 1: (h_a=0.75, α_0=30°, a=1/3, M_∞=0.1)

Table 1 and Table 2 show the comparison of the time-averaged thrust coefficient and propulsion efficiency computed by the present RANS solver with the available Euler [6] and Navier – Stokes [20] results respectively. The highest time-averaged thrust coefficient of 0.7219 with a propulsion efficiency of 61.34% is obtained. Fig. 6 represents the coefficient of lift, drag and moment versus the non-dimensional time for the five consecutive cycles. The Mach number contour at different instants of time for one complete cycle of flapping motion of the aerofoil is plotted in Fig. 7.

TABLE 1
THRUST COEFFICIENT VALUES FOR CASE 1

Reduced frequency k	Phase angle Φ	Present (RANS)	Euler [6] nviscid	Euler [6] Friction corrected	Navier-Stokes [20]
0.67	75°	0.3535	0.491	0.478	0.52
0.78	90°	0.7219	0.863	0.850	Not available

TABLE 2
PROPULSION EFFICIENCY VALUES FOR CASE 1

Reduced frequency k	Phase angle Φ	Present (RANS)	Euler [6] nviscid	Euler [6] Friction corrected	Navier-Stokes [20]
0.67	75°	65.89%	78.6%	76.5%	87%
0.78	90°	61.34%	64.5%	63.5%	Not available

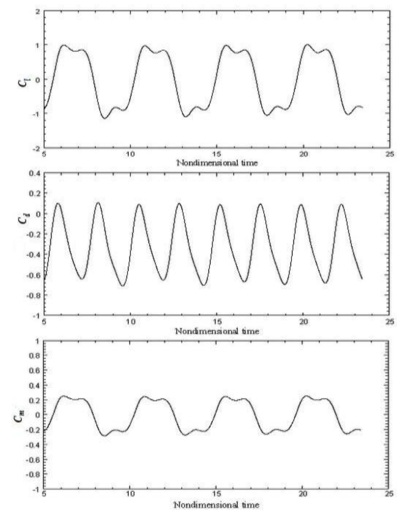

Fig.6. The coefficient of lift, drag and moment versus the non dimensional time for five cycles at h=0.75, α0=30°, a=1/3, M∞=0.1, k=0.67, Φ=75°.

Case 2: (h_a = 1.0, α_0 = 4°, a = 1/4, Φ = 90°, M_∞ = 0.3)

The time-averaged thrust coefficient and propulsion efficiency obtained by the present calculations are listed in Table 3 and Table 4 along with the Euler solutions of Yang et al. [6] and Neef et al. [21] respectively. In these cases, the highest time-averaged thrust coefficient is 0.197 with a propulsion efficiency of 80.5% is obtained. Fig. 8 shows the coefficient of unsteady surface pressure distribution for NACA 0012 aerofoil for one complete cycle. The corresponding pressure contour plots at different instants of time for one complete cycle of flapping motion of the aerofoil is shown in Fig. 9.

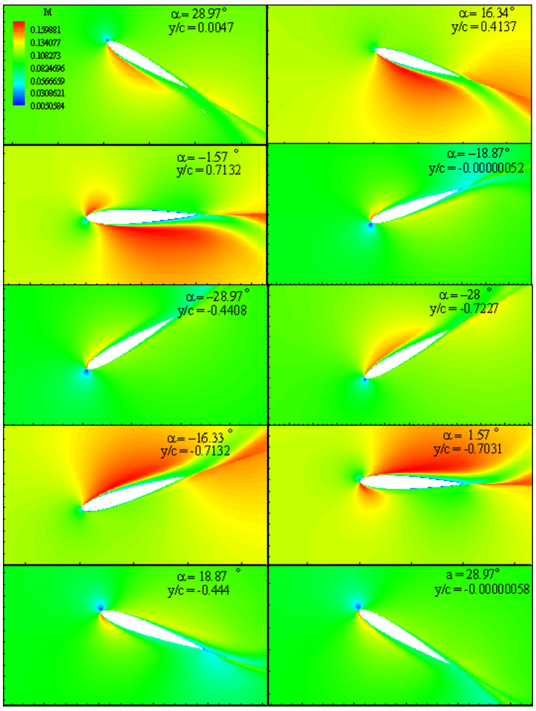

Fig.7. The Mach number contour at different instants of time for one cycle of flapping motion of aerofoil at h=0.75, α0=30°, a=1/3, M∞=0.1, k=0.67, Φ=75°.

TABLE 3
THRUST COEFFICIENT VALUES FOR CASE 2

Reduced frequency k	Phase angle Φ	Present (RANS)	Euler (Yang et al. [6])	Euler (Neef et al. [21])
0.1	90°	0.05604	0.0681	0.048
0.172	90°	0.16065	0.197	Not Available

TABLE 4
PROPULSION EFFICIENCY VALUES FOR CASE 2

Reduced frequency k	Phase angle Φ	Present (RANS)	Euler (Yang et al. [6])	Euler (Neef et al. [21])
0.1	90°	88.08%	89.5%	89%
0.172	90°	77.77%	80.5%	Not Available

6. CONCLUDING REMARKS

The lift, pitching moment, thrust coefficient and propulsion efficiency for a combined pitching and plunging NACA 0012 aerofoil has been computed by the Implicit Reynolds-averaged Navier-Stokes (IMPRANS) solver. In case1, the time-averaged thrust coefficient of 0.7219 with a propulsion efficiency of 61.34% is obtained. In case 2, the higher time-averaged thrust coefficient of 0.197 with a propulsion efficiency of 80.5% is obtained. From the above results we can conclude that the highest propulsion efficiency and the highest thrust coefficient do not occur at the same reduced frequency, higher efficiency usually occurs at lower reduced frequency and higher thrust coefficient occurs at higher reduced frequency.

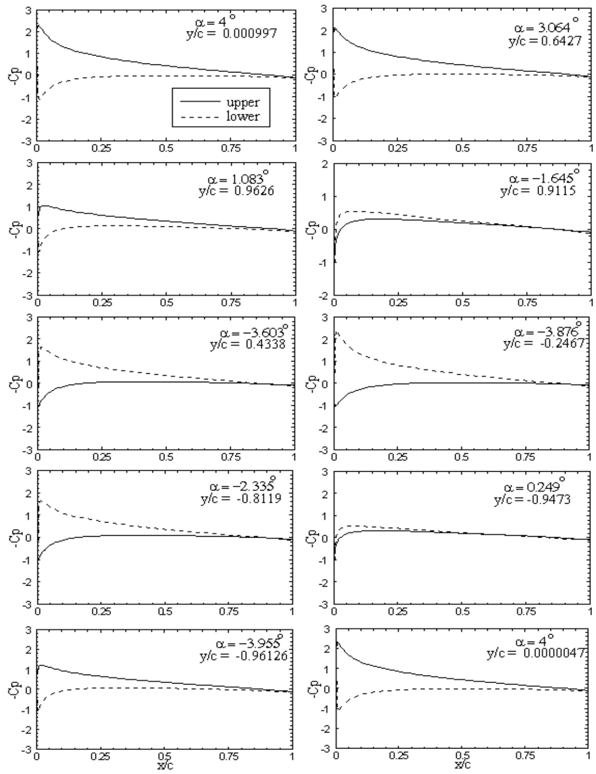

Fig.8. The coefficient of unsteady surface pressure distribution on the NACA 0012 aerofoil for one complete cycle at h=1.0, α0=4°, a=1/4, M∞=0.3, k=0.1, Φ=90°.

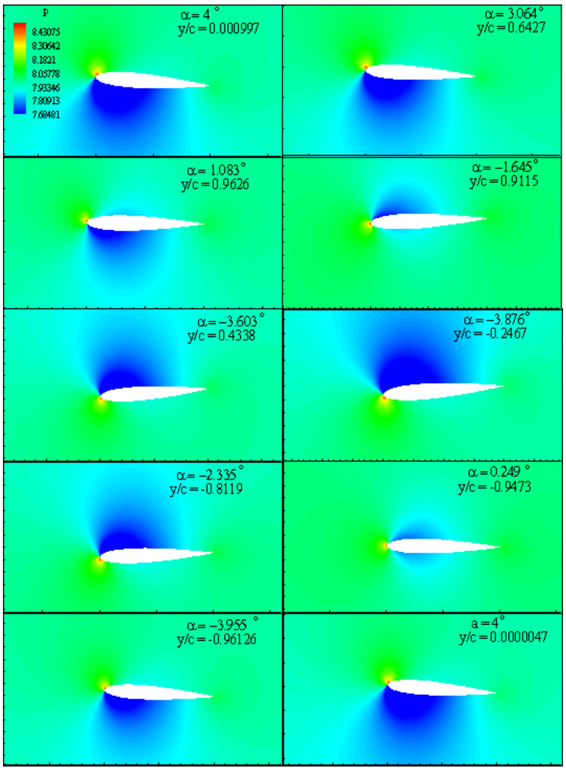

Fig.9. The pressure contour at different instants of time for one cycle of flapping motion of aerofoil at h=1.0, α0=4°, a=1/4, M∞=0.3, k=0.1, Φ=90°.

7. PARAMETER INDEX TABLE

α_o	Amplitude of pitching oscillation
α_m	Mean angle of attack
$\alpha(t)$	Instant angle of attack or incidence
$\dot{\alpha} / U_\infty$	Non-dimensional pitching velocity
γ	Ratio of specific heats
λ, μ	Viscosity coefficients
μ_∞	Free stream viscosity
μ_t	Turbulent viscosity coefficient
ρ_∞	Free stream density
τ	Non-dimensional time
ω	Non-dimensional angular frequency
$Ø$	Phase angle between pitching and plunging motion
Γ	Boundary curve
Ω_{ij}	Control volume surrounding the nodal point (i, j) of the curvilinear grid
Δt	Real or physical time step
c	Aerofoil chord
e	Energy
f	Pitch or plunge physical frequency
h_a	Non-dimensional amplitude in plunge
h_{ij}	Area of quadrilateral
k	Non-dimensional reduced frequency
n	Time level
p	Pressure
t	Physical time
u, v	Velocity components
x, y	Cartesian coordinates
y_o	Amplitude of plunge or heave
$y(t)$	Instant Plunge distance of the aerofoil
y / U_∞	Non-dimensional plunging velocity
A, B, R, S	Jacobian matrices
C_d	Drag coefficient
C_t	Thrust coefficient
C_p	Surface pressure coefficient
C_l	Lift coefficient
C_m	Moment coefficient
F, G	Inviscid flux vectors
V, W	Viscous flux vectors
M_∞	Free stream Mach number
Pr	Prandtl number
Re_∞	Free stream Reynolds number
U	Vector of conserved variables
U_∞	Free stream velocity

REFERENCES

[1] D. G. Mabey, "Unsteady Aero-dynamics: Restrospect and prospect," *Aero-nautical Journal*, Vol. 103, No. 1019, Review Paper No. 003, 1 – 18, 1999.

[2] W. J. McCroskey, Unsteady airfoils, *Ann. Rev. Fluid Mech.*, Vol. 14, 285 - 311, 1982.

[3] W. J. McCroskey, "Some Rotorcraft Applications of Computational Fluid Dynamics," NASA TM 100066, 1988.

[4] W. Shyy, M. Berg and D. Lyungvist, "Flapping and Flexible Wings for Biological and Micro Air Vehicles," *Progress in Aerospace Sciences*, Vol. 35, No. 5, pp. 455 – 505, 1999.

[5] T. J. Mueller (ed.), "Fixed and Flapping Wing Aerodynamics for Micro Air Vehicles," *Progress in Aeronautics and Astronautics, AIAA*, Reston, VA, Vol. 195, 2001.

[6] S. Yang, S. Luo and F. Liu, "Optimization of Unstalled Pitching and Plunging Motion of an Airfoil," 44th *AIAA Aerospace Sciences Meeting and Exhibit*, Reno, Nevada, 1055, 2006.

[7] T. Theodorsen,"General theory of aerodynamic instability and the mechanism of flutter," *NACA Report No. 496*, 1934.

[8] I. E. Garrick, "Propulsion of a flapping and oscillating airfoil," *NACA Report No. 567*, 1936.

[9] I. H. Tuncer and M. F. Platzer, "Computational study of flapping airfoil Aerodynamics," *Journal of Aircraft*, Vol. 37, pp. 514 – 520, 2000.

[10] K. Isogai, Y. Shinmoto and Y Watanabe, "Effects of Dynamic Stall on Propulsive Efficiency and Thrust of Flapping Airfoil," *AIAA Journal*, Vol. 37, pp. 1145-1151, 1999.

[11] R. Ramamurti and W. Sandberg, "Simulation of Flow about Flapping Airfoils using Finite Element Incompressible Flow Solver," *AIAA Journal*, Vol. 39, pp. 253-260, 2001.

[12] J. M. Anderson, K. Streitlien, D. S. Barrett and M. S.Triantafyllou, "Oscillating foils of high propulsive efficiency," *J. Fluid Mech*., 360, pp. 41 - 72, 1998.

[13] R. M. Beam and R. F. Warming, "An Implicit Factored Scheme for the Compressible Navier-Stokes Equations," *AIAA Journal*, Vol. 16, No. 4, pp. 393 – 402, 1978.

[14] M. G. Hall, "Cell Vertex Multi-grid Scheme for Solution of the Euler Equations," RAE-TM-Aero 2029, *Proc. Conf. on Numerical methods for fluid dynamics*, pp. 303 – 345, 1985.

[15] A. Jameson, W. Schmidt and E. Turkel, "Numerical Solution of Euler Equations by Finite Volume Methods Using Runge Kutta Time Stepping Schemes," *AIAA Paper* 81-1259, 1981.

[16] Sharanappa V. Sajjan, Vimala Dutta and P. K. Dutta "Numerical Simulation of flow over pitching bodies using an implicit Reynolds-averaged Navier-Stokes solver," *Proc. of 12th Asian congress of Fluid Mechanics*, Daejeon, Korea, 2008.

[17] Vimala Dutta, Sharanappa and P. K. Dutta, "Navier - Stokes Computations for a Helicopter Rotor Blade in Hover," *Proc. 8th Annual CFD Symposium, CFD Division of Aeronautical Society of India*, Bangalore, CP 18, 2005.

[18] Sharanappa V. Sajjan, Vimala Dutta, and P. K. Dutta, "Viscous Unsteady Flow around a Helicopter Rotor Blade in Forward Flight," *Proc. 9th Annual CFD symposium, CFD Division of Aeronautical Society of India*, Bangalore, 2006.

[19] P. K. Dutta, Vimala Dutta, and Sharanappa V. Sajjan. "RANS Computation of Flow past Wind Turbine Blades," *Proc. of 7th Asian Computational Fluid Dynamics Conference*, Bangalore (Invited Paper), 2007.

[20] J. M Anderson, "Vorticity control for efficient propulsion," *PhD Thesis*, Massachusetts Institute of Technology and Woods Hole Oceanographic Institution, 1996.

[21] M. F. Neef and D. Hummel, "Euler solutions for a finite-span flapping wing," *Tech. rep., Conference on fixed, flapping and rotary wing vehicles at very low Reynolds numbers*, University of Norte Dame, IN. 2000.

Available online at:
http://tsest.org/index.php/TCMS/article/view/29

Download full text article at:
http://tsest.org/index.php/TCMS/article/download/29/10

Cite this work as:
K. Siva Kumar and Sharanappa V. Sajjan, "Unsteady Flow past a Flapping Aerofoil" *TSEST Transaction on Control and Mechanical Systems*, Vol. 1, No. 1, PP. 43-48, May, 2012.